Transactions of the **13th International Conference on Structural Mechanics in Reactor Technology** (SMiRT 13), Escola de Engenharia - Universidade Federal do Rio Grande do Sul, Porto Alegre, Brazil, August 13-18, 1995

# Determination of the impulsive response of elastoplastic plates and shells by means of discrete element models

Iturrioz, I., Riera, J.D.
*Universidade Federal do Rio Grande do Sul, CPGEC, Porto Alegre, RS, Brazil*

ABSTRACT:The determination of the dynamic response of elastoplastic plate and shell structures is carried out employing a discrete representation of the continuum, associated with an explicit integration scheme in the time domain. Comparisons with experimental results attest to the accuracy and reliability of the proposed method.

## 1 INTRODUCTION

The determination of the response of shell structures subjected to dynamic loads that produce large displacements requires considerable effort. In such cases, an approach based on a discret model (DEM), in conjunction with an explicit integration scheme in the time domain, besides its intrinsic simplicity, has shown to be extremely competitive (Riera & Iturrioz, 1995). In previous applications by Hayashi (1982), Riera (1984) and Rocha & Riera (1990), the solids under consideration were assumed to fail in tension (fracture). In order to extend the approach to thin shell structures, it was deemed important to evaluate first the performance of the method in elastoplastic, isotropic and homogeneous shells, without fracture (Riera & Iturrioz, 1995). In this paper, the authors present additional case studies, introducing a procedure to insure that at any given point in the loading process, chosen by the analyst, plastic deformations take place without further volume change.

## 2 DISCRETE REPRESENTATION OF LAMINAR STRUCTURES

The model employed is based on the representation of a continuum by means of an array of nodal masses interconnected by unidimensional massless elements. The cubic array shown in Fig.(1) was adopted, consisting of a cubic cell with 8 nodal points at the vertices plus a central node, each with three degrees of freedom. The masses are linked by longitudinal and diagonal elements of lenghs $L_C$ and $\sqrt{3}L_C/2$, respectively. The equivalence between an orthotropic elastic solid with the principal axes of orthotropic oriented in the direction of the longitudinal elements and the cubic model was shown by Nayfeh & Heftzy (1978) within the framework of linear elasticity. The equations of motion of the resulting system with $N$ degrees of freedom can be expressed in the form:

$$M\vec{u} + \vec{f} = \vec{Q}(t) \tag{1}$$

In which $M$ denotes the (diagonal) mass matrix, $\vec{u}$ the vector of generalized coordinates (nodal displacements), $\vec{f}$ the restitutive and dissipative nodal forces, which may be dependent on present and past nodal displacements and $\vec{Q}(t)$ the external forces. In linear, elastic systems $\vec{f} = K\vec{u}$, $K$ being the stiffness matrix. If the system presents viscous dissipative forces (Newton damping), eq (1) becomes:

$$M\vec{u} + C\vec{u} + \vec{f} = \vec{Q}(t) \tag{2}$$

When $C = \alpha M$, the system (2) way be numerically integrated in the time domain by means of the explicit central finite difference algorithm . Since nodal coordinates can be updated at each integration step, the approach allows the consideration of large displacements, i.e. geometrical nonlinearities.

The stiffness of the elements depends on the local elastic properties of the solid, and on the lenght $L_C$ of the basic cell. In many problems, it is possible to generate a mesh of nodal coordinates, starting from a cubic array, by means of conformal mapping. Since conformal mapping preserves orthogonality, the cubic cells are only slightly distorted. It is then admitted that the expressions for the stiffness maintain their validity, provided that the actual lenght $L_C$ or $\left(\sqrt{3}L_C/2\right)$ of each element is used in its calculation. Nodal masses, in turn, must be transformed according to the law:

$$transformed\,mass = (detJ)\,original\,mass \tag{3}$$

in which $(detJ)$ denotes the jacobian of the transformation calculated at the node under consideration.

In applications to laminar structures, it is necessary to include at least one cell throughout the thickness, which means that nodal masses must be retained on the upper and lower, as well as in the middle surface. On account of the missing elements at the interior nodes in the direction normal to the middle surface, the stiffness in this direction is slightly reduced, but the effect has no perceptible influence in usual situations. Of course, it is a straight-forward matter to use more than a single layer accros the shell thickness.

## 3 YIELD SURFACE FOR A SINGLE LAYER SHELL

In the examples described in this paper, it is was assumed that the material is linearly elastic-perfectly plastic, that is, no strain hardening or fracture were considered. Since the results are compared with solutions based on conventional plasticity theory, the effective yield surface for membrane excitation of the discrete model was determined with Tresca's criteria for a homogeneous shell of the same thickness as shown in fig.(2). It may be seen that, by adopting a yield strain for the elements equal to the experimental yield strain in uniaxial tension, Tresca's failure criterion is recovered in two quadrants, tension-tension and compression-compression. The model predicts higher strenghts in the other quadrants, where it is closer to the Von Mises yield surface.

## 4 EXAMPLES

A circular cylindrical shell tested by Morino & Leech under an impulsive load generated by an explosive pad located on part of its surfaces was analysed as Example 1. The dimensions and relevant mechanical properties of the structure are indicated in fig.(3).

A normal pressure was applied on the upper shell surface. The load amplitude $q_s$ was determined by equating the total impulse within the time of load application $t_d$, which in turn was adopted equal to the time needed by a compression wave to travel through the shell thickness, that is, $t_d = c_p L_c$, where $c_p = \sqrt{E/\sigma}$. The shell is considered fixed along all four borders, condition that may not have been fully satisfied by the experimental set up. However, insufficient information was available to evaluate the flexibility of the real supports. The loaded region covered a 60° section of the shell, which presents a total opening equal to 120°. The shell was made of Aluminium alloy 6061-T6, which is characterized by a very week strain hardening and may be approximated by the elastic-perfectly plastic model. A single cell was used throughout the thikness, while 100 elements were disposed in the longitudinal and 25 in circumferential directions, totalling 23000 degrees of freedom. Only half the shell was representated, on account of symmetry.

Fig.(4) shows the vertical displacements at points $A$ and $B$. The global correlation of the present formulation with the experimental curve, as well as with the solution of Argyris 'et al' (1990) is excelent. Slight discrepancies for point $B$ may be due, as indicated before, to nonzero rotations at the shell supports. Finally , fig.(5) shows the deformed configuration at $t = 0.375ms$, when the displacement at $A$ reaches its maximum value. In this analysis, as reported by Riera & Iturrioz (1995), no volumetric deformation control was used.

Example 2 consist of the determination of the dynamic response of the cylindrical shell with the geometric and mechanical properties indicated in fig.(6), also due to impulsive loading. The shell was tested by Lindeberg & Kennedy (1975), who measured the total impulse applied on the structure as approximately 15000 $Ns/m^2$. The impulsive load results in an initial velocity, considered uniform in the longitudinal direction, while in the circumferential direction varies as shown in Fig (6). Due to the symmetry only half of the shell was modelled, assuming also plane strain conditions. The resulting DEM model, presented 476 nodal points.

The experimental results are compared with predictions of the present formulation, and with a finite element solution due to Ishizaki & Bathe (1980). Fig.(7) shows the evolution with time of the radial displacement for $\phi = 15°$, measured from the vertical y-axis. The circunferential strain at $\phi = 0°$ vs. time is plotted in fig. (8). In every case, the predictions of the DEM model are quite close to the experimental results. The goodness of fit of both numerical solutions (DEM and FEM) are equivalent.

## 5 VOLUMETRIC CONTROL IMPLEMENTATION

In the first applicatons of the model to elastoplasticity, element deformations were not subjected to any restriction, which in case of large strains, especially in the case of negative volumetric strains, led to poor predictions. An option to prevent volumetric strains from changing after any predetermined stage in the loading process, was introduced in the calculation scheme. This control is performed on the basic tetrahedron, as shown in fig.(9) The control mechanism is activated whenever any two bars of the tetrahedron are already in the plastic range, insuring that yielding occurs under constant volume, and includes the following tasks:

a)Define the position of the center of gravity of the tetrahedron $\vec{g}(g_1, g_2, g_3)$

b)As indicated in fig.(9) , determine the versors $\vec{i}, \vec{j}, \vec{k}, \vec{l}$ ,with origin at the tetrahedron vertices and oriented towardss its center of gravity

c)Let $V_\phi$ denote the volume of the tetrahedron before deformation, $V_\phi(\alpha)$ the volume of a tetrahedron geometrically similar to the deformed tetrahedron, of volume $V_{def}$:

$$V_{\phi'}(\alpha) = V_{def} + \Delta Vol(\alpha) \tag{4}$$

The scalar $\alpha$ must be altered until the volume change $\Delta Vol(\alpha)$ is such that $V_\phi = V_{\phi'}(\alpha)$. The value of $\alpha$ thus determined is the factor that, multiplying the versors $\vec{i}, \vec{j}, \vec{k}$ and $\vec{l}$, leads to the corrected position of the nodal points. The bisection method is employed in the search for $\alpha$. The final position of each nodal point is finaly determined by evaluating the resultant of the versors corresponding to all tetrahedrons from which the node is a common vertex. At each time integration step this procedure may be repeated, using a sucessive approximations approach.

Although the approach described has not been extensively tested, and may still undergo improvements, it has already been verified that in problems of large displacements but small deformations, volume control exerts only a marginal influence on the results. Thus, the response in Examples 1 and 2 is essentially unchanged when volume control is activated. In problems involving large deformations, on the other hand, it considerably extends the range of applicability of the DEM as fomulated herein. As a final example 3, Fig.(10) presents a comparison of the experimental and computed deformed configurations of an aluminium bar that impacted with a velocity of 216 $m/s$ against a rigid wall inclined 4° with respect to the direction of impact. The experimental results are reported by Zukas (1982), where additional information on the tests may be found. Although the circular bar was modelled by a square section with the same area, the correlation is quite satisfactory. In this case, with no volume control, the model completely fails.

## 6 CONCLUSIONS

An extension of a discrete element representation of solid media, to model elasto-plastic laminar structures subjected to short duration loadings was discussed in the paper. The approach offers significant advantages on account of its simplicity, facility of implementation and efficiency when used in vectorial computers. Moreover, it may also be employed to study fracture and local effects under impact loading, which would require only an increase in the number of cells across the thickness. The examples shown indicate that the model is able to satisfactorily predict the geometrically nonlinear response of elastoplastic laminar structures, both in case of predominant membrane or bending action. Moreover, a control of volumetric deformations is proposed, allowing the consideration of large deformation problems.

## REFERENCES

Argyris, J., Balmer, H. J. & Doltisinis, I. 1990. A Simple But Subtle Model for Analysis of Shell-Like Structures, Computer Methods in Applied Mechanics and Engineering 85,(pp1-20), North Holland.

Balmer, L. M. 1964. Theorical - experimental correlation of large dynamic and permanent deformations of impulsively loaded simple structure, Research and Tech. Div., Wright - Patterson AFB, Rept.FDL-TDR-(pp64-104).

Hayashi, Y. 1982. Sobre um modelo de discretização de estruturas tridimensionais aplicado em dinâmica não linear. Tese M.Sc., CPGEC, Universidade Federal do Rio Grande do Sul, Porto Alegre, Dez.

Morino, L., Leech, J. W. & Witmer, E. A. 1971.An improved Numerical Calculation Technique for Large Elastic-Plastic Transient Deformations of Thin shells. Journal of Applied Mechanics. June,(pp429-439)ASME, N. Y.

Nayfeh, A. H. & Hefzy, M. S. 1978. Continuum modeling of three dimensional truss-like space structures. AIAA Journal, 16(8):(pp779-787).

Lindberg, H. E. & Kennedy, T. C. 1975. Dynamics Plastic pulse Buckling Beyond Strain-Rate Reversal, Journal of Applied Mechanics, Trans.ASME , (pp.411-416).

Riera, J. D. 1984. Local effects in impact problems on concrets structures. Proceedings, Conference on Structural Analysis and Design of Nuclear Power Plants, Porto Alegre, Brasil, Oct., CPGEC/UFRGS, Porto Alegre V. III, (pp57-79).

Riera, J. D. & Iturrioz, I. 1995. Discrete elements dynamic Response of Elastoplastic Shells subjected to impulsive Loading, Communications in Numerical Methods in Engineering, to be published, Ed Lewis, R. W. & Carey, G. F., Wiley & Sons, U.K.

Rocha, M. M. 1989. Ruptura e Efeito de Escala em Materias não Homogeneos. Tese M. Sc., CPGEC, Universidade Federal do Rio Grande do Sul, Brasil, Set.

Rocha, M. M. & Riera, J. D. 1990. On size effects and rupture of nonhomogeneos materials.In Proceedings, Congress in Fracture Processes in Concrete, Rock and Ceramics, Eds. J. G. M. Van Mier, J. G. Rots & A. Bakker, Chapman & Hall/Ed.Fn Spon, London, (pp451-460).

Zukas, J. A. 'et al' 1982. Impact Dynamics. ch 2, (pp29-53), John Wiley & Sons, U.S.A.

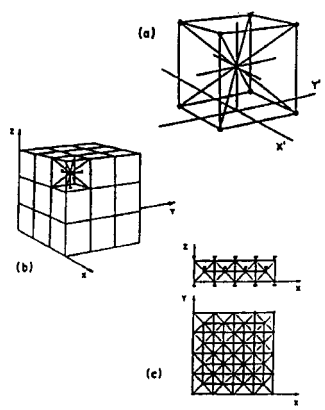


Figure 1: Cubic Structure of *Nayfeh & Heftzy*(1978) model. a) Basic cubic model. b) and c) Composition of prisms.

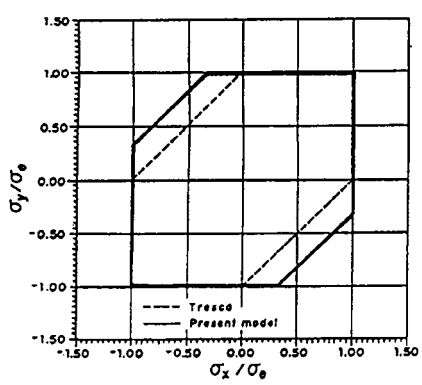


Figure 2: Comparison beteween Tresca and DEM Yield Surface.

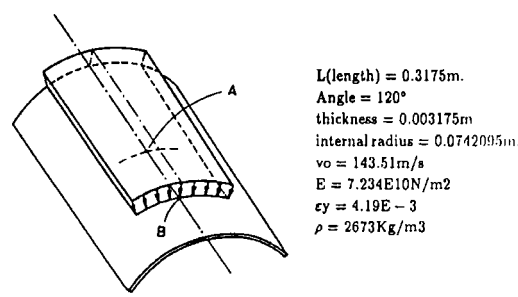


Figure 3: Geometrical and Mechanical properties for Example 1 (Shell Structure)

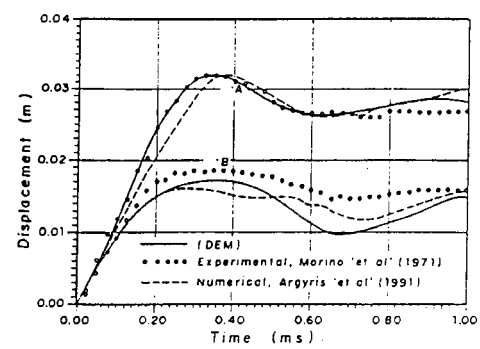


Figure 4: Comparison of numerical and experimental normal displacements vs. time curves, for points A and B in the shell Structure.

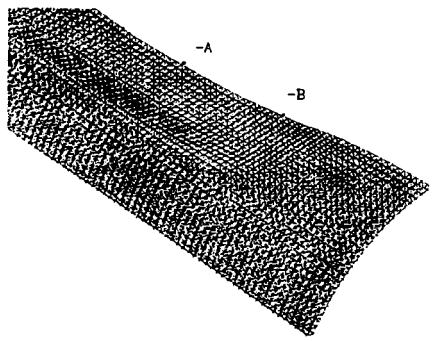


Figure 5: Detail of deformed configuration of the shell at $t = 0.375ms$.

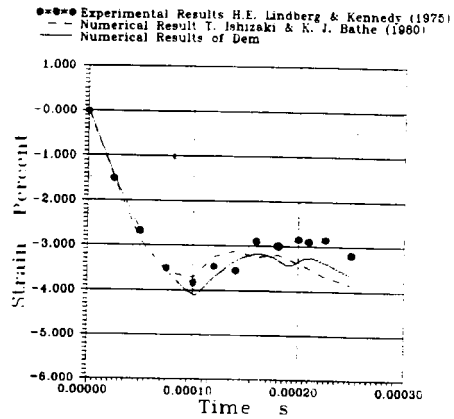


Figure 8: Comparison of experimental and numerically determined circumferential strains at $\phi = 0°$ vs. time for the elastoplastic cylindrical shell.

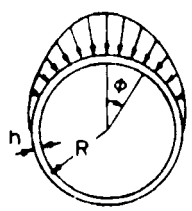


R = 0.1525m.
h = 0.051m.
PlaneStrainAnalysis
E = 5.89E10N/m2
$\nu = 0.33$
Et/E = 0.023
$\rho$ = 2730Kg/m3

Figure 6: Layout of the Elastoplastic cilindrical Shell with geometrical and mechanical properties (Lindberg & Kennedy 1975).

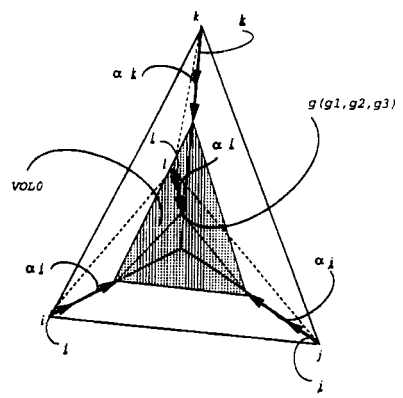


Figure 9: Layout of elemental tetrahedrom.

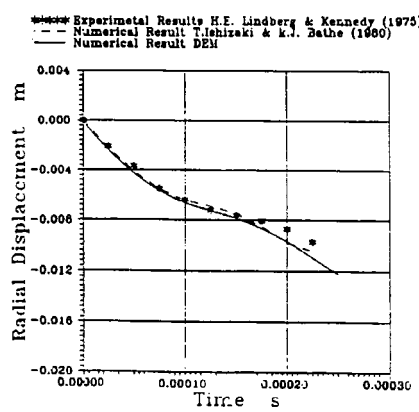


Figure 7: Comparison of the experimental and numerical radial displacements vs. time of the elastoplastic cilindrical shell.

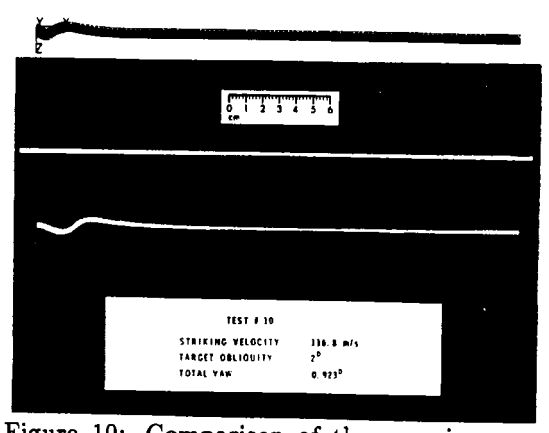


Figure 10: Comparison of the experimental and numerical final configuration on the long rods that impact over the target (Zukas 1982).